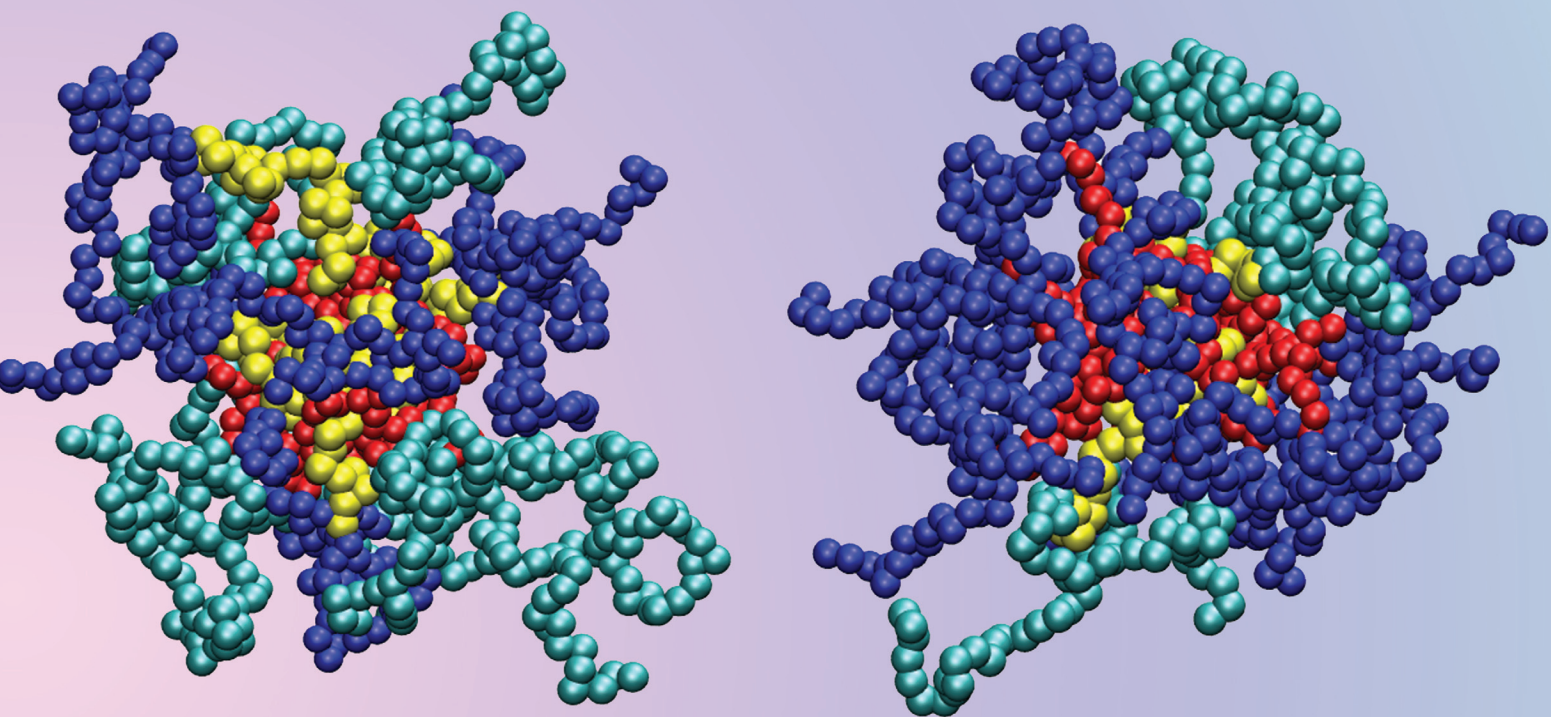
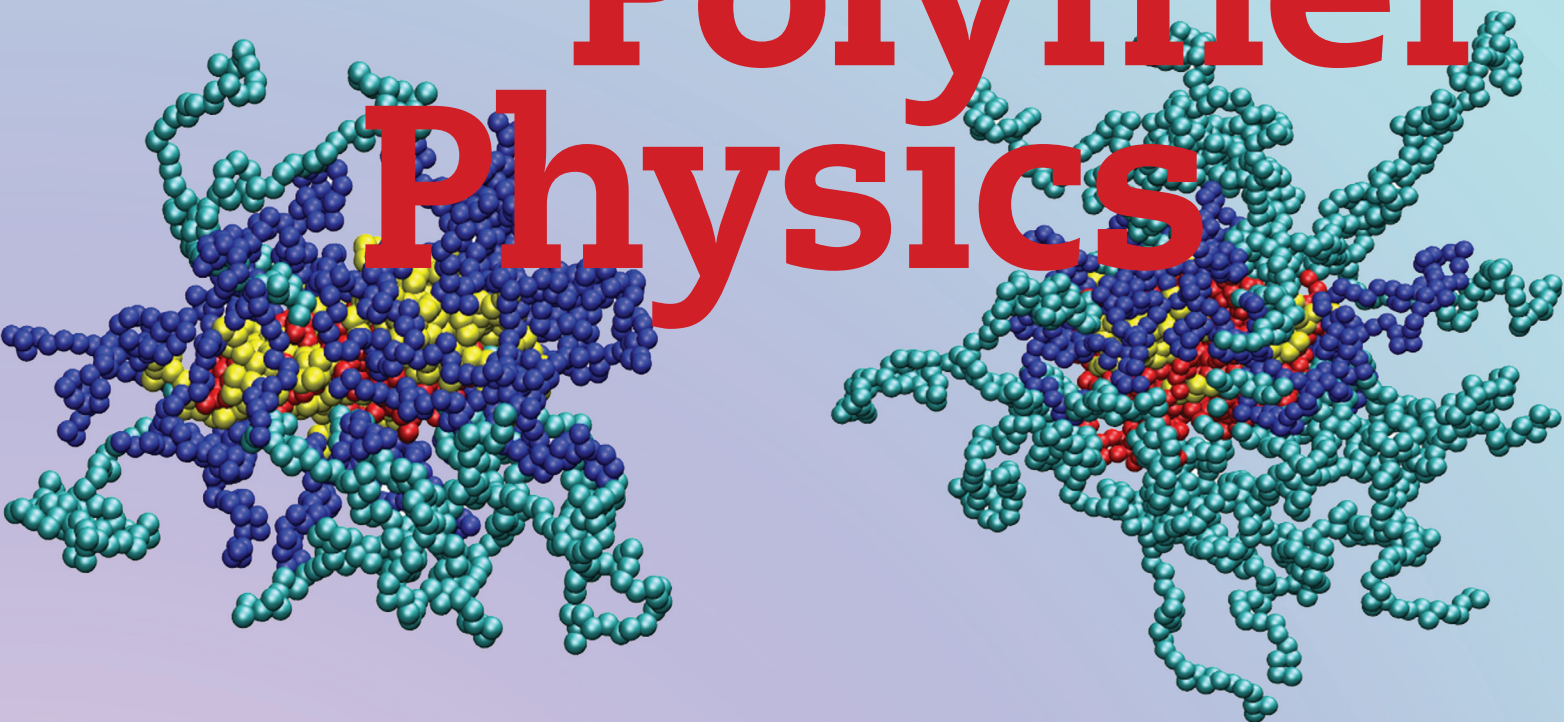


JOURNAL OF POLYMER SCIENCE | PART B

# Polymer Physics

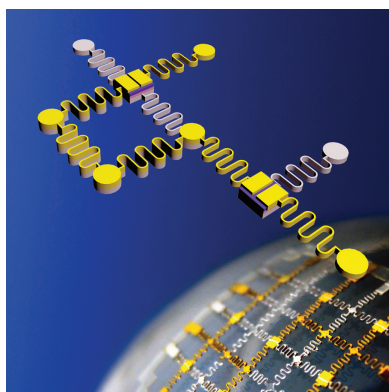


VOL 53 NO 6 | 15 MARCH 2015

[WWW.POLYMERPHYSICS.ORG](http://WWW.POLYMERPHYSICS.ORG)

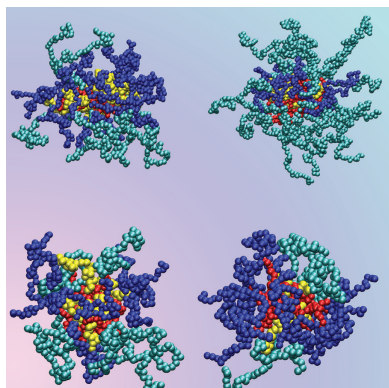
WILEY

# Polymer Physics



## PHOTOPOLYMERIZATION

Ju-Hyung Kim, Moon Jong Han, and Soonmin Seo present a technique for realizing an electrical circuit composed of organic devices on a highly flexible, stretchable, and patchable freestanding substrate, using an UV-curable polymer. Each organic device composing a circuit array is fabricated on a small individual polymeric plate, and connected to neighboring devices using polymeric bridges. The report on page 453, details how each polymeric bridge is formed in a spring shape, and shows high flexibility and stretchability, providing an excellent platform for the transference of electrical signals. Furthermore, the UV-curable polymer has intrinsic adhesive properties, which enable the mounting of freestanding polymeric substrate onto non-flat surfaces, with conformal contact.



## SELF-ASSEMBLY

The cover shows snapshots of mixed micelles formed by chemically identical linear/star and star/star copolymer mixtures obtained from molecular dynamics simulations. On page 442, Othonas Moutos, Leonidas N. Gergidis, Andreas Kalogirou, and Costas Vlahos report that architectural asymmetry between chains induces effective interactions. The effective interactions cause a small decrease in the aggregation number of preferential micelles in linear/star mixtures, triggering the non-random mixing between the solvophilic moieties in the corona for all mixtures.

**Coming soon** Look for these important papers in upcoming issues of JPS: Polymer Physics

**Xue Liu, Yang Shao, Si-Yuan Lu and Ke-Fu Yao**

**High-accuracy Bulk Metallic Glass Mold Insert for Hot Embossing of Complex Polymer Optical Devices**

DOI: 10.1002/polb.23670

**Carlos G. Lopez, Sarah E. Rogers, Ralph H. Colby, Peter Graham and João T. Cabral**

**Structure of Sodium Carboxymethyl Cellulose Aqueous Solutions: A SANS and Rheology Study**

DOI: 10.1002/polb.23657

**Christian H. Hofmann, Sebastian Grobelny, Pawel T. Panek, Laura K. M. Heinen, Ann-Kristin Wiegand, Felix A. Plamper, Christoph R. Jacob, Roland Winter, Walter Richtering**

**Methanol-Induced Change of The Mechanism of the Temperature- and Pressure-Induced Collapse of N-Substituted Acrylamide Copolymers**

DOI: 10.1002/polb.23676

All our articles are available online in advance of print. The articles listed here have been judged by either the referees or the editor to be very important, and were immediately copyedited, proofread and published online. As long as there is no page number available, online manuscripts should be cited in the following manner: Authors, *J. Polym. Sci. Part B: Polym. Phys.*, online publication date, DOI

# Entropic Effects in Mixed Micelles Formed by Star/Linear and Star/Star AB Copolymers

Othonas Moulτος,<sup>1,2</sup> Leonidas N. Gergidis,<sup>3</sup> Andreas Kalogirou,<sup>1</sup> Costas Vlahos<sup>1</sup>

<sup>1</sup>Department of Chemistry, University of Ioannina, 45110, Greece

<sup>2</sup>Chemical Engineering Program, Texas A&M University at Qatar, Doha 23874, Qatar

<sup>3</sup>Department of Materials Science and Engineering, University of Ioannina, 45110, Greece

Correspondence to: C. Vlahos (E-mail: cvlahos@cc.uoi.gr)

Received 29 September 2014; revised 24 November 2014; accepted 24 November 2014; published online 00 Month 2014

DOI: 10.1002/polb.23654

**ABSTRACT:** The entropic effects in the comicellization behavior of amphiphilic AB copolymers differing in chain architecture of solvophilic A or solvophobic B parts are studied by means of molecular dynamics simulations. In particular, we studied linear/star and star/star copolymer mixtures. The properties of interest were the critical micelle concentration, the mean aggregation number, the shape of the micelle, which is expressed by the shape anisotropy, the thickness of the corona, and the solvophobic core radius. We found that the critical micelle concentration values for linear/star and copolymer mixtures show a positive deviation from the analytical predictions of the molecular theory of comicellization for

chemically identical copolymers. This could be attributed to the effective interactions between copolymers originated from the architectural asymmetry. The effective interactions induce a small decrease in the aggregation number of preferential micelles in linear/star mixtures triggering the nonrandom mixing between the solvophilic moieties in the corona for all mixtures. © 2014 Wiley Periodicals, Inc. *J. Polym. Sci., Part B: Polym. Phys.* **2014**, *00*, 000–000

**KEYWORDS:** block copolymers; self-assembly; simulations; star polymers

**INTRODUCTION** In recent years, there is an increased interest in studying the entropic effects, arising from the architecture and size asymmetry of polymer species, in the structure and the properties of polymer mixtures.<sup>1–12</sup>

Mackay et al.<sup>1</sup> conducted several experiments in order to study the miscibility of linear polystyrene (PS) in the presence of spherical cross-linked PS and dendritic polyethylene (PE) nanoparticles. They observed that although linear PS-linear PE blends are phase separated system, branched PE nanoparticles disperse uniformly in PS. This means that both architecture and size asymmetry make a clear difference in the miscibility of this system. They found that thermodynamically stable dispersion of nanoparticles into polymeric matrix was enhanced when the radius of gyration of the linear polymer is greater than the radius of the nanoparticle.

Foster and coworkers<sup>2–6</sup> studied chemically identical blends of star and linear PS<sup>2,3</sup> and the respective star/linear blends of polybutadiene<sup>4</sup> (PB) and poly(methyl methacrylate)<sup>5</sup> (PMMA). By deuterating one of the components they were able to measure the effective Flory interaction parameter  $\chi_{eff}$  arising from size and architecture asymmetry of polymer chains, through small-angle neutron scattering experiments.

They found that in PS and PMMA blends with stars having up to 12 arms,  $\chi_{eff}$  always increased when the number of arms and the length of linear chains were increased. The effective interactions lead to nonrandom mixing of linear and star chains. Experimentally, phase separation is observed in two particular PB and PMMA blends with six and seven arms and sufficiently large linear chains.<sup>4,5</sup>

Vlahos and coworkers<sup>7–10</sup> studied the effects of the size and chain architecture on the miscibility of both heteropolymer<sup>8,10</sup> and chemically identical<sup>7–9</sup> star/star, star/linear, and linear/linear blends using Renormalization Group Theory and Monte Carlo simulations. By calculating the Flory parameter  $\chi_{eff}$  and the stability conditions they found that the heteropolymer star/linear blends are more miscible than linear/linear ones at least for short chains. With the increase in the number of arms, the miscibility was significantly enhanced. They suggested that this mainly originates from the shielding effect of the star cores, which reduces the number of heterocontacts. In contrast, the chemically identical star/linear blends are less miscible compared with the linear/linear blends. The excluded volume interactions between units belonging to different chains are not canceled as Flory's theory suggests but remain leading in nonrandom mixing or even demixing in some

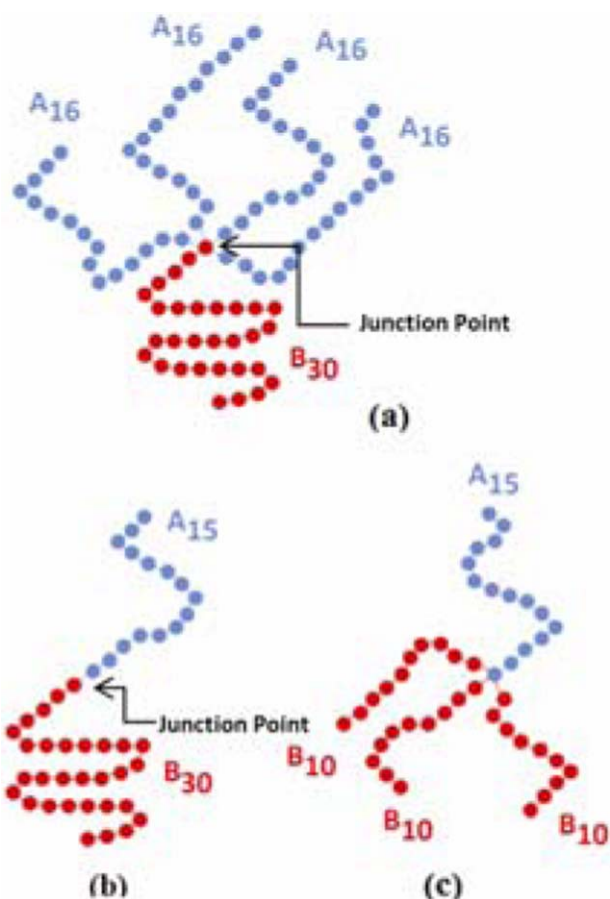


**FIGURE 1** Cartoon representation of (a) miktoarm star copolymer  $(A_{16})_4B_{30}$ , (b) linear diblock copolymers  $A_{15}B_{30}$ , and (c) miktoarm star copolymer  $A_{15}(B_{10})_3$ . [Color figure can be viewed in the online issue, which is available at [wileyonlinelibrary.com](http://wileyonlinelibrary.com).]

circumstances. Nonidealities arising from size asymmetry between chemically identical chains were also observed in concentrated mixed solutions.<sup>11</sup>

Dong et al.<sup>12</sup> studied the self-assembly of Janus nanoparticles in block copolymer scaffolds. They found that the Janus nanoparticles do not take symmetric distribution in the lamella interface of asymmetric block copolymers. The deviation of nanoparticles from interface is attributed to asymmetric interactions from the block segments and the unconventional entropic effect at the molecular scale.

To the best of our knowledge, results on the entropic effects arising from the architecture and size asymmetry of copolymers in mixed micelles are lacking. In this article, we employed molecular dynamics simulations, with Langevin thermostat, to elucidate the effect of the copolymer architecture on the micellization behavior of copolymers mixtures. In particular, we studied linear/star and star/star mixtures (Fig. 1). The properties of interest are the critical micelle concentration cmc, the mean aggregation number  $N_p$ , the shape of the micelle, which is expressed by the shape anisotropy  $\kappa^2$ , the thickness of the corona  $H$  and the solvophobic core radius  $R_c$ .

## MODEL

We employed a coarse-grained model to represent the amphiphilic copolymer chains used in this study. A group of atoms was modeled as a bead with diameter  $\sigma$ . Bead-bead interactions were calculated by means of a truncated Lennard-Jones potential:

$$U_{LJ}(r_{ij}) = \begin{cases} 4\epsilon \left[ \left( \frac{\sigma}{r_{ij}} \right)^{12} - \left( \frac{\sigma}{r_{ij}} \right)^6 - \left( \frac{\sigma}{r_{cij}} \right)^{12} + \left( \frac{\sigma}{r_{cij}} \right)^6 \right], & r_{ij} \leq r_{cij} \\ 0, & r_{ij} > r_{cij} \end{cases} \quad (1)$$

where  $\epsilon$  is the well-depth, and  $r_{cij}$  is the cutoff radius. Different beads were connected with finitely extensible nonlinear elastic bonds (FENE). A key physical characteristic of polymer molecules is that the chains cannot cross. The FENE potential inherently achieves this being harmonic at its minimum, while the bonds cannot be stretched beyond a maximum length determined by  $R_0$ . The FENE potential is expressed as

$$U_{\text{Bond}}(r_{ij}) = \begin{cases} -0.5kR_0^2 \ln \left[ 1 - \left( \frac{r_{ij}}{R_0} \right)^2 \right], & r_{ij} \leq R_0 \\ \infty, & r_{ij} > R_0 \end{cases} \quad (2)$$

where  $r_{ij}$  is the distance between beads  $i$  and  $j$ ,  $k = 25T\epsilon/\sigma^2$  and  $R_0$  is the maximum extension of the bond ( $R_0 = 1.5\sigma$ ). These parameters<sup>13</sup> prevent chain crossing by ensuring an average bond length of  $0.97\sigma$ . The solvent molecules are considered implicitly. The short timesteps needed to model solvent's behavior (the fast motion) restrict the timescales that maybe sampled, thereby limiting the information that can be obtained for the slower motion of the copolymer. Molecular dynamics simulation with Langevin thermostat allows the statistical treatment of the solvent, incorporating its influence on the copolymer by a combination of random forces and frictional terms. The friction coefficient and the random force couple the simulated system to a heat bath and therefore the simulation has canonical ensemble (NVT) constraints. The equation of motion of each bead  $i$  of mass  $m$  in the simulation box follows the Langevin equation:

$$m_i \ddot{\mathbf{r}}_i(t) = -\nabla \sum_j [U_{LJ}(r_{ij}) + U_{\text{Bond}}(r_{ij})] - m_i \zeta \dot{\mathbf{r}}_i(t) + \mathbf{F}_i(t) \quad (3)$$

where  $m_i$ ,  $\mathbf{r}_i$ , and  $\zeta$  are the mass, the position vector, and the friction coefficient of the  $i$  bead, respectively. The friction coefficient is equal to  $\zeta = 0.5\tau^{-1}$ , with  $\tau = \sigma\sqrt{m/\epsilon}$ . The random force vector  $\mathbf{F}_i$  is assumed to be Gaussian, with zero mean, and satisfies the equation

$$\langle \mathbf{F}_i(t) \cdot \mathbf{F}_j(t') \rangle = 6k_B T m \zeta \delta_{ij} \delta(t-t') \quad (4)$$

$k_B$  is the Boltzmann constant and  $T$  is the temperature. In amphiphilic copolymers A, beads are considered solvophilic and B beads solvophobic. In every conducted simulation the solvophobic part B contained 30 beads, while the length of

the A block varied. The individual constituents of the mixtures are (a) linear diblock copolymers with 63 and 16 solvophilic beads denoted as  $A_{63}B_{30}$  and  $A_{16}B_{30}$ , respectively (b) miktoarm star copolymers with 63 solvophilic beads, which are distributed in one  $A_{63}$ , two  $(A_{32})_2$ , or three branches  $(A_{21})_3$  and 30 solvophobic units distributed in one  $B_{30}$  or three branches  $(B_{10})_3$ . Some of the aforementioned copolymer architectures are illustrated in Figure 1.

Three binary mixtures of copolymers were studied in this work. Namely, the mixture of (i) linear  $A_{63}B_{30}$  diblock copolymer with star  $(A_{21})_3B_{30}$ , (ii) star  $(A_{32})_2B_{30}$  with star  $(A_{16})_4B_{30}$  and (iii) linear  $A_{63}B_{30}$  with star  $A_{63}(B_{10})_3$ . The chosen ratio of solvophobic to solvophilic units  $\gamma$  allows the systems to equilibrate faster and thus save computational time.

The molar fractions of the two individual constituents in the mixture,  $[X_1]$  and  $[X_2]$ , are given by

$$[X_1] = \frac{N_1}{N_1 + N_2} \quad (5)$$

$$[X_2] = 1 - [X_1] \quad (6)$$

where  $N_1$  and  $N_2$  are the number of chains of the two different copolymers in the mixture. In every case studied we had  $[X_1] = 1, 0.75, 0.5, 0.25,$  and  $0$  while  $[X_2]$  values were set, respectively, according to eq 6. The total copolymer concentration,  $[X]$ , is given by

$$[X] = \frac{N_1 M_1 + N_2 M_2}{V} \quad (7)$$

where  $M_1$  and  $M_2$  are the molecular weights of copolymers of type 1 and 2, respectively, and  $V$  is the total volume of the simulation box.

Molecular dynamics simulations with Langevin thermostat were performed in a cubic box with periodic boundary conditions, using the open-source massive parallel simulator LAMMPS.<sup>14</sup> Previous works have proved the high efficiency of LAMMPS in the study of amphiphilic copolymers.<sup>15–18</sup> The reduced temperature of the simulation  $T^*$  was set to  $T^* = k_B T / \varepsilon = 1.8$ . This choice of temperature allows the studied systems to have both micelles and free molecules.<sup>15</sup> If the temperature is very low, the studied system contains only aggregates and no free molecules; while if the temperature is very high, the studied system contains only free molecules and no aggregates. Different cutoff distances in the Lennard-Jones potential were used<sup>15–18</sup> to describe the interactions between copolymer units. The B-B interaction had an attractive potential with cutoff radius  $r_{cij} = 2.5 \sigma$  while the A-A and A-B interactions were considered repulsive and have cutoff radii  $r_{cij} = 2^{1/6} \sigma$ . In the latter case, the Lennard Jones potential is shifted by  $\varepsilon$ . For the sake of simplicity, all types of beads were considered to have the same mass ( $m = 1$ ) and diameter ( $\sigma = 1$ ). Copolymers were assumed to reside to the same micelle if the distance between any two non-bonded solvophobic beads B, belonging to different chains,

was found within  $1.5 \sigma$ . The aforementioned criterion has been adopted by the literature for the description of the micellization process where this distance corresponds to the maximum extension of the FENE bonds.<sup>13</sup> In all simulations, we set  $\varepsilon = 1$ .

In this study, systems containing  $N_1 + N_2 = 125$  copolymer chains were simulated for the calculation of the cmc values. All other properties were computed from systems with  $N_1 + N_2 = 1000$  chains at total copolymer concentration  $[X] = 0.12$  where most aggregates are formed.<sup>15</sup> The system size was chosen so to prevent the largest micelles from having a radius of gyration greater than the one-fourth of the box side length. The use of the one quarter of the simulation box side proved to be a sufficient condition to avoid interaction of chains and micelles with their images. No system size effects were observed for all the calculated quantities reported on this article.

To avoid bond crossing at the desired concentration, copolymer chains of types 1 and 2 were initially arranged on a lattice box. The energy of the chains was minimized and then the lattice box was replicated to obtain the desired number of chains. We performed one million time steps with integration step  $\Delta t = 0.008 \tau$  setting all cutoff radii equal to  $r_{cij} = 2^{1/6} \sigma$  to eliminate any bias introduced from the initial conformation. Then, the system was allowed to equilibrate for 10 million steps. The simulation was subsequently conducted for 10 million steps for the systems with 125 copolymer chains, and 100–500 million steps for the larger systems with 1000 amphiphiles. The duration of the simulation was evaluated by calculating the tracer autocorrelation function:

$$C(t) = \frac{\langle N(t_0 + t)N(t_0) \rangle - \langle N(t_0) \rangle^2}{\langle N^2(t_0) \rangle - \langle N(t_0) \rangle^2} \quad (8)$$

where  $N(t)$  is the number of molecules in the micelle in which the copolymer resides at time  $t$ . We took all copolymers as tracers, and every time step as a time origin  $t_0$ . The characteristic relaxation time  $t_{\text{relax}}$  is defined as the required time for  $C(t)$  to reach the value<sup>15</sup> of  $e^{-1}$ . In Figure 2, we report the tracer autocorrelation function for different systems. Each simulation was conducted for at least  $10 t_{\text{relax}}$  to have 10 independent conformations. The properties of interest were calculated as averages from 1000 to 2000 snapshots for the systems with 125 to 1000 chains, respectively.

The equilibration in coarse-grained MD simulations for micellization of surfactants suffers from difficulty of convergence as has been reported in the literature.<sup>19</sup> Diblock copolymers with larger molecular weights  $A_{15}B_{30}$  need 500 million steps to equilibrate.<sup>15</sup> By increasing the length of the solvophilic part the equilibration time progressively decreases and this justifies the use the  $A_{63}B_{30}$  linear diblock copolymer with such a long A block.<sup>15</sup> The effect of the complex architecture in reducing equilibration times is dominant. Micelles formed by star copolymer chains equilibrate faster compared to micelles formed by linear chains.<sup>16</sup> This is due to the steric interactions between branches in the micelle's

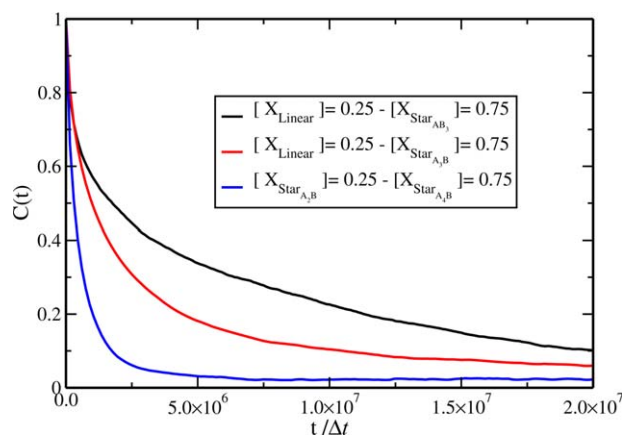


**FIGURE 2** Tracer autocorrelation function  $C(t)$  for different copolymer mixtures. [Color figure can be viewed in the online issue, which is available at [wileyonlinelibrary.com](http://wileyonlinelibrary.com).]

corona, which guide the star chains to bail out from the micelle easier resulting in the faster relaxation. In addition, blending the linear with star copolymers the time needed for equilibration decreases as the star content in the mixture increases (Fig. 2). Similarly, copolymers containing solvopho-

bic part with star architecture equilibrates faster than the respective linear diblock copolymers.<sup>20</sup>

## RESULTS AND DISCUSSION

### Critical Micelle Concentration

Critical micelle concentration (cmc) is an important property of self-assembly because it is a direct measure of the thermodynamic stability of the micelles in the solution. In general, amphiphilic copolymers with lower cmc values are stable at lower concentration. The onset of micellization is traditionally depicted by plotting the free (nonassociated) copolymer monomers concentration  $[F]$  as a function of the total copolymer monomers concentration  $[X]$ . For ideal systems as  $[X]$  increases, small micelles are formed and the concentration of free chains reduces progressively reaching a plateau at the cmc. For higher copolymer concentration  $[X]$  the nonidealities introduced by the excluded volume interactions reduce the free chain concentration and the maximum value of  $[F]$  defines the cmc for real systems.<sup>15</sup> In the case of amphiphilic copolymer mixtures, where mixed aggregates are formed, the maximum of the total free chain concentration including both types of copolymers determines the cmc. Figure 3 shows plots of the total free copolymer

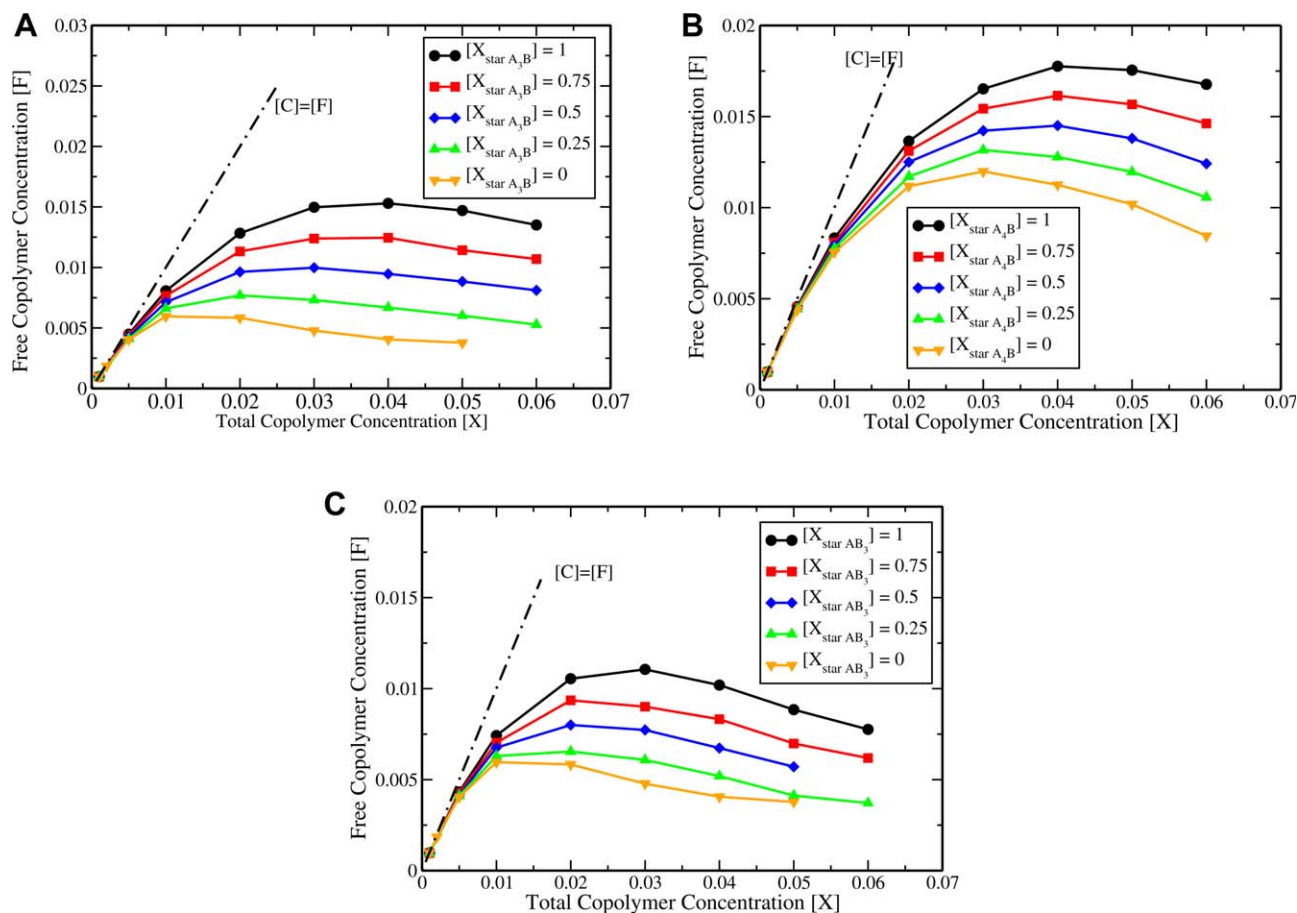


**FIGURE 3** Plots of the total free copolymer concentration against the total copolymer concentration  $[X]$  for the simulated binary mixtures of (a) linear  $A_{63}B_{30}$ /star  $(A_{21})_3B_{30}$ , (b) star  $(A_{32})_2B_{30}$ /star  $(A_{16})_4B_{30}$ , and (c) linear  $A_{63}B_{30}$ /star  $A_{63}(B_{10})_3$  at different molar fractions of two types of amphiphilic copolymers. [Color figure can be viewed in the online issue, which is available at [wileyonlinelibrary.com](http://wileyonlinelibrary.com).]

**TABLE 1** Critical Micelle Concentration (cmc) Values for Different Copolymer Mixtures

Mixture	$M_w$	$\gamma$	cmc
Linear $A_{63}B_{30}/\text{Star}(A_{21})_3B_{30}$	93	0.48	
$[X_{(A_{21})_3B_{30}}] = 1$			0.0153
$[X_{(A_{21})_3B_{30}}] = 0.75$			0.0125
$[X_{(A_{21})_3B_{30}}] = 0.5$			0.0100
$[X_{(A_{21})_3B_{30}}] = 0.25$			0.0077
$[X_{(A_{21})_3B_{30}}] = 0$			0.0060
Star $(A_{32})_2B_{30}/\text{Star}(A_{16})_4B_{30}$	94	0.47	
$[X_{(A_{16})_4B_{30}}] = 1$			0.0178
$[X_{(A_{16})_4B_{30}}] = 0.75$			0.0161
$[X_{(A_{16})_4B_{30}}] = 0.5$			0.0145
$[X_{(A_{16})_4B_{30}}] = 0.25$			0.0132
$[X_{(A_{16})_4B_{30}}] = 0$			0.0120
Linear $A_{63}B_{30}/\text{Star}A_{63}(B_{10})_3$	93	0.48	
$[X_{A_{63}(B_{10})_3}] = 1$			0.0111
$[X_{A_{63}(B_{10})_3}] = 0.75$			0.0094
$[X_{A_{63}(B_{10})_3}] = 0.5$			0.0080
$[X_{A_{63}(B_{10})_3}] = 0.25$			0.0065
$[X_{A_{63}(B_{10})_3}] = 0$			0.0060

concentration against the total copolymer concentration  $[X]$  for the simulated binary mixtures of linear  $A_{63}B_{30}/\text{star}(A_{21})_3B_{30}$ , star  $(A_{32})_2B_{30}/\text{star}(A_{16})_4B_{30}$ , and linear  $A_{63}B_{30}/\text{star}A_{63}(B_{10})_3$  at different molar fractions of two types of amphiphilic copolymers. The cmc values calculated from Figure 3 are given in Table 1. The molecular theory for the formation of micelles can be used to describe qualitatively the trends of these values.<sup>19</sup> According to the theory the driving force of aggregation is the change in the Gibbs free energy  $g_{\text{mic}}$  associated with the transfer of  $n$  unimers from the solution to a micelle. The higher the  $g_{\text{mic}}$  the higher the cmc value. For uncharged copolymers  $g_{\text{mic}}$  can be modeled as the sum of four different terms that takes into account all of the free energy changes that occur upon micelle formation<sup>21</sup>  $g_{\text{mic}} = g_{\text{tr}} + g_{\text{int}} + g_{\text{pack}} + g_{\text{st}}$ . The first three terms are related to the solvophobic part of the copolymer, and the fourth is associated with the solvophilic counterpart. The free energy of transfer  $g_{\text{tr}}$  reflects the energy change associated to the transfer of the solvophobic block from the solution to micelles core. The interfacial free energy  $g_{\text{int}}$  takes into account the energy change upon the formation of the interface between the core and the solution while  $g_{\text{pack}}$  involves the free energy change associated with constraining the end or ends of the solvophobic part to lie at the periphery of micelle core. The last term  $g_{\text{st}}$  accounts for the contribution of steric interactions between the solvophilic units of the copolymers. The cmc value of pure linear diblock copolymer  $A_{63}B_{30}$  is 0.006 and is lower than that of pure star  $(A_{21})_3B_{30}$ , which is 0.0153. Both copolymers have the same molecular weight and the same solvophilic/solvophobic ratio. However, in the pure micelles formed by the

linear diblock copolymers the steric interactions between linear blocks in the solvophilic corona are smaller compared with the respective interactions between the three solvophilic arms of miktoarm copolymer  $(A_{21})_3B_{30}$ . Thus,  $g_{\text{mic}}$  in linear copolymers is lower than the respective of miktoarm stars, leading in lower cmc value. In the case of mixtures of linear and miktoarm copolymers snapshot analysis revealed the formation of mixed micelles. The small aggregates initially formed by linear chains, which later on are enriched with miktoarm copolymers. The steric penalty needed to overcome for transferring a free miktoarm star chain from the solution to a mixed micelle is smaller compared with the respective  $g_{\text{st}}$  for the insertion of a free miktoarm star chain in a small aggregate, formed by pure miktoarm star copolymer chains. Thus, the formation of mixed micelles is thermodynamically favored with  $g_{\text{mic}}$  values lying between the respective values of pure linear and pure star micelles. This leads to the increase of cmc values of the mixture with respect to the pure linear copolymer solution. As expected the cmc of the mixture increases as the molar fraction of star chains increases (Table 1). A quantitative prediction of the cmc of the mixture in terms of cmc of pure constituents is given by means of the molecular theory of comicellization. The cmc of the binary mixed system  $C_M$  can be obtained as<sup>22,23</sup>

$$\frac{1}{C_M} = \frac{[X_1]}{f_1 C_1} + \frac{1-[X_1]}{f_2 C_2} \quad (9)$$

where  $C_1$  and  $C_2$  are the cmc of the type 1 and type 2 copolymers and  $f_1, f_2$  are the activity coefficients of the amphiphilics taking into account the nonideality of the interactions between molecules of different types.<sup>24</sup> In ideal mixtures, the activity coefficients for both components are equal to unity. The cmc values of the linear  $A_{63}B_{30}/\text{star}(A_{21})_3B_{30}$  mixture for star copolymer molar fraction  $[X_{\text{star}}] = 0, 0.25, 0.5, 0.75,$  and  $1$  are illustrated in Figure 4(a). In the same figure, the analytical results obtained from eq 9 with unity activity coefficients are also presented. It can be observed that there is a small deviation from the ideal behavior, which increases as the molar fraction of miktoarm star copolymer increases. The simulation results revealed the presence of effective interactions, between chemically identical copolymers. Both linear and star copolymers contain the same solvophobic part, which is a linear chain with 30 beads, the nonidealities should originate from the solvophilic corona. In the case of linear/star mixtures, effective interactions take place between the linear block and the chemically identical star with three arms.

In Figure 5, the number density  $\rho(r)$  of the beads belonging to the mixed micelle is illustrated as a function of the distance from the micelle center of mass. For the reported mixtures with  $(\langle Rg^2 \rangle_{\text{core}})^{1/2}$  almost equal to  $5\sigma$  (Table 2), the melting of the solvophobic core leads the solvophilic beads residing in the vicinity of the interface ( $5\sigma < r < 12\sigma$ ), to come very close having high density. As we mentioned in the introduction Vlahos and Kosmas<sup>7-9</sup> using renormalization group theory have shown that the architectural and the size asymmetry in chemically identical homopolymer blends

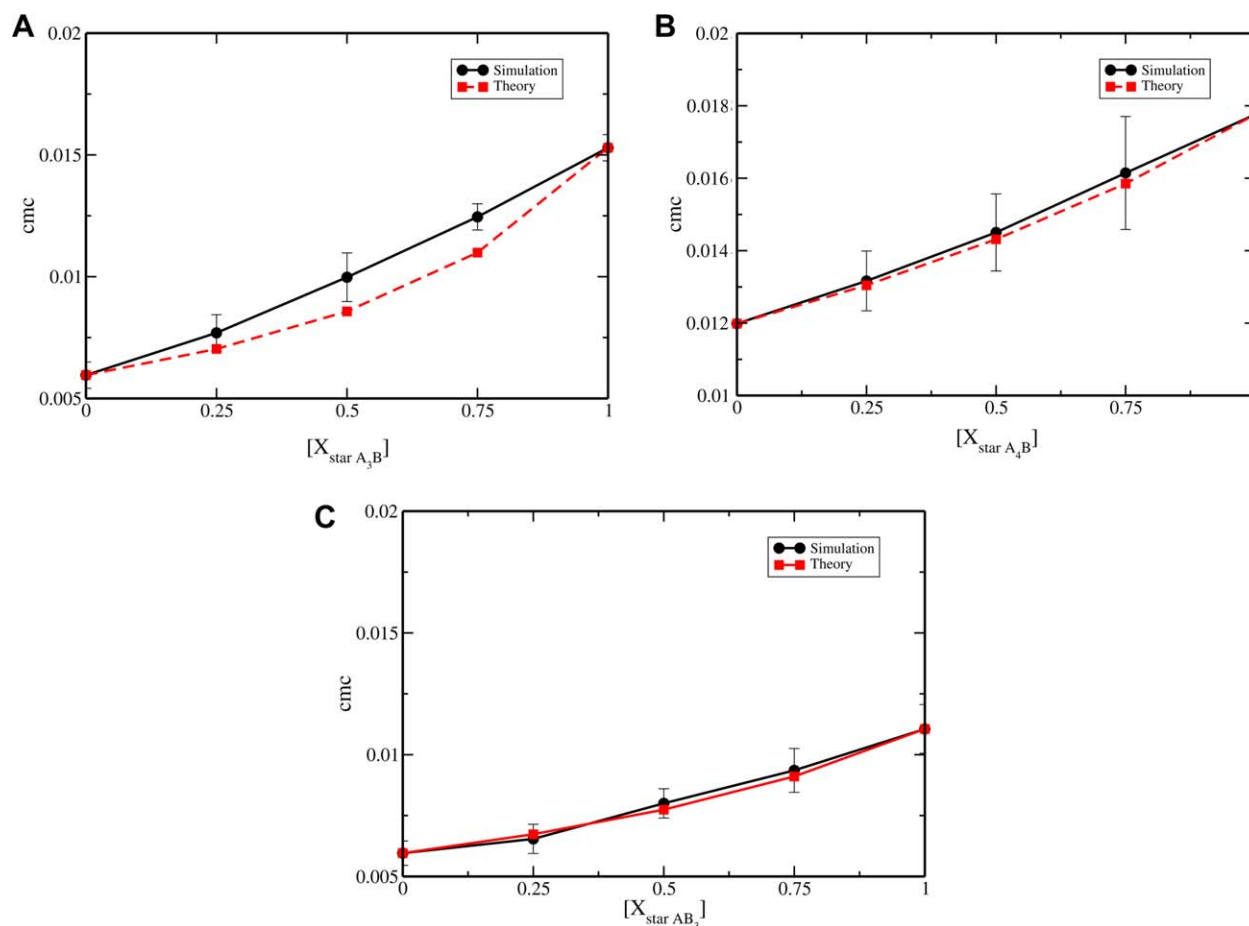


**FIGURE 4** Plots of the cmc values of (a) linear  $A_{63}B_{30}$ /star  $(A_{21})_3B_{30}$  mixture for star copolymer molar fraction. (b) Star  $(A_{32})_2B_{30}$ /star  $(A_{16})_4B_{30}$  mixtures with respect to molar fraction of star copolymer  $(A_{16})_4B_{30}$  and (c) linear  $A_{63}B_{30}$ /star  $A_{63}(B_{10})_3$  mixtures. Within the same figure, the analytical results obtained from eq 9 with unity activity coefficients are also shown. [Color figure can be viewed in the online issue, which is available at [wileyonlinelibrary.com](http://wileyonlinelibrary.com).]

induce nonidealities. The effective Flory parameter  $\chi_{\text{eff}}$  describing such interactions, in star/star chemically identical blends increases when the difference between the numbers of arms of two different species increases, obtaining the highest values when the star chain of the one component becomes a linear polymer<sup>4</sup> (star/linear blends). In addition, Vlahos and Kosmas<sup>9</sup> found that  $\chi_{\text{eff}}$  also increases as the molecular weight of both polymers decreases. Thus, the deviation from the ideal behavior in linear  $A_{63}B_{30}$ /star  $(A_{21})_3B_{30}$  mixture may be ascribed in the architectural asymmetry of solvophilic parts of amphiphilic copolymers.

In the case of star  $(A_{32})_2B_{30}$ /star  $(A_{16})_4B_{30}$  mixtures the variation of cmc with respect to molar fraction of star copolymer  $(A_{16})_4B_{30}$  is presented in Figure 4(b). It can be observed that the cmc of pure star copolymer  $(A_{16})_4B_{30}$  with four solvophilic arms is higher than the respective of pure star  $(A_{32})_2B_{30}$ . Again, the reason is the higher steric penalty needed to be overcome for transferring a free miktoarm star chain with four solvophilic arms from the solution to a pure micelle of  $(A_{16})_4B_{30}$  copolymers. Mean cmc values of the mixture for any molar fraction  $[X_{\text{star}}(A_{16})_4B_{30}]$ ,

despite the great standard deviation, are almost identical with the theoretical values indicating negligible nonidealities induced by the architectural asymmetry of two

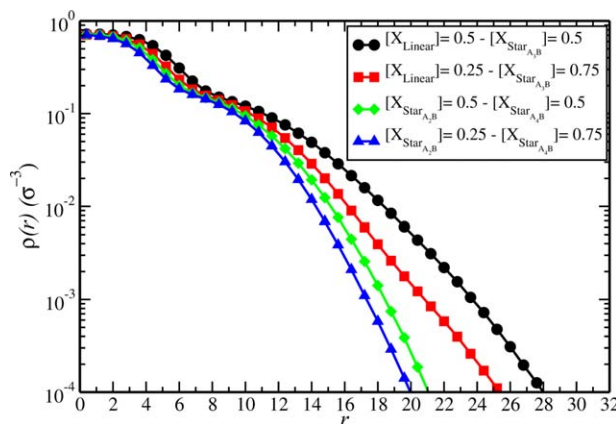


**FIGURE 5** Plot of the number density  $\rho(r)$  for different copolymer mixtures. [Color figure can be viewed in the online issue, which is available at [wileyonlinelibrary.com](http://wileyonlinelibrary.com).]

**TABLE 2** Shape Characteristics of the Most Probable Formed Aggregates of Various Mixtures

System	$N_p$	$\langle Rg^2 \rangle_{\text{micelle}}$	$\langle Rg^2 \rangle_{\text{core}}$	$\langle \kappa^2 \rangle_{\text{micelle}}$	$\langle \kappa^2 \rangle_{\text{core}}$	$H$	$R_{\text{core}}$
<b><math>A_{63}B_{30} - (A_{21})_3B_{30}</math></b>							
$[X (A_{21})_3B_{30}] = 1$	11	77.7 (0.2)	22.4 (0.1)	0.038 (0.001)	0.106 (0.002)	5.27 (0.02)	6.11 (0.01)
$[X (A_{21})_3B_{30}] = 0.75$	16	105.1 (0.5)	26.4 (0.2)	0.0359 (0.0006)	0.088 (0.002)	6.59 (0.04)	6.62 (0.03)
$[X (A_{21})_3B_{30}] = 0.50$	22	133 (1)	30.3 (0.3)	0.028 (0.001)	0.074 (0.004)	7.75 (0.07)	7.1 (0.03)
$[X (A_{21})_3B_{30}] = 0.25$	28	157.4 (0.9)	33.6 (0.2)	0.0215 (0.0005)	0.065 (0.004)	8.71 (0.05)	7.48 (0.02)
$[X (A_{21})_3B_{30}] = 0$ [Ref. 3]	38	191 (2)	39.7 (0.7)	0.015 (0.003)	0.05 (0.01)	9.7 (0.1)	8.13 (0.07)
<b><math>(A_{32})_2B_{30} - (A_{16})_4B_{30}</math></b>							
$[X (A_{16})_4B_{30}] = 1$	9	68.4 (0.3)	21.5 (0.2)	0.050 (0.001)	0.112 (0.002)	4.69 (0.04)	5.98 (0.03)
$[X (A_{16})_4B_{30}] = 0.75$	11	78.6 (0.3)	23.2 (0.3)	0.041 (0.001)	0.109 (0.003)	5.22 (0.05)	6.21 (0.04)
$[X (A_{16})_4B_{30}] = 0.50$	13	88.3 (0.3)	24.3 (0.1)	0.0334 (0.0008)	0.097 (0.003)	5.76 (0.03)	6.36 (0.01)
$[X (A_{16})_4B_{30}] = 0.25$	15	97.4 (0.3)	25.4 (0.1)	0.0285 (0.0009)	0.090 (0.002)	6.23 (0.02)	6.50 (0.01)
$[X (A_{16})_4B_{30}] = 0$	17	106.1 (0.4)	26.3 (0.3)	0.025 (0.001)	0.082 (0.004)	6.67 (0.05)	6.62 (0.04)
<b><math>A_{63}B_{30} - A_{63}(B_{10})_3</math></b>							
$[X A_{63}(B_{10})_3] = 1$	22	147.3 (0.5)	34.9 (0.4)	0.030 (0.001)	0.0150 (0.005)	8.04 (0.05)	7.62 (0.04)
$[X A_{63}(B_{10})_3] = 0.75$	28	163.5 (0.7)	36.3 (0.3)	0.021 (0.001)	0.103 (0.004)	8.72 (0.05)	7.77 (0.03)
$[X A_{63}(B_{10})_3] = 0.50$	31	172.0 (0.4)	36.1 (0.3)	0.0188 (0.0008)	0.075 (0.004)	9.17 (0.03)	7.76 (0.02)
$[X A_{63}(B_{10})_3] = 0.25$	35	183 (1)	37.4 (0.3)	0.016 (0.001)	0.059 (0.005)	9.57 (0.07)	7.89 (0.03)
$[X A_{63}(B_{10})_3] = 0$ (Ref. 3)	38	191 (2)	39.7 (0.7)	0.015 (0.003)	0.05 (0.01)		

Standard deviation is inside the parentheses.

branches between star copolymers  $(A_{32})_2B_{30}$  and  $(A_{16})_4B_{30}$ . According to the molecular theory of comicellization<sup>22–24</sup> the activity coefficients  $f_1$  and  $f_2$  are given by the relations  $f_1 = \exp[u(1 - [X_1])^2]$ ,  $f_2 = \exp(u[X_1]^2)$  where  $u$  is the interaction parameter between units of different copolymers. By taking into account eq 9 and the expressions for the activity coefficients  $f_1$  and  $f_2$  we extract parameter  $u$  by fitting the simulation values of  $1/C_M$ . We obtain  $u = 0.1$  for star  $(A_{32})_2B_{30}$ /star  $(A_{16})_4B_{30}$  and  $u = 0.6$  for the linear  $A_{63}B_{30}$ /star  $(A_{21})_3B_{30}$  mixtures. These results are in agreement with the aforementioned predictions of Vlahos and Kosmas<sup>7–9</sup> for star/star blends.

Next, we study linear  $A_{63}B_{30}$ / star  $A_{63}(B_{10})_3$  mixtures where the constituent copolymers differ in the architecture of solvophobic part. The cmc value of pure star  $A_{63}(B_{10})_3$  copolymer is higher than the respective value of the linear diblock copolymer [Fig. 4(c)]. The solvophobic units of star tailed copolymer  $A_{63}(B_{10})_3$  are constrained near the point of connection with solvophilic block. Thus, the creation of larger interface, with the solvent molecules, leads to a larger interfacial energy and consequently to higher cmc.<sup>20</sup> Furthermore, the concentration of the units, close to the point of connection hinders, their interactions with other solvophobic units to reduce the free energy.<sup>20</sup> For copolymer mixtures, as can be seen from Figure 4(c), the ideal model of eq 9 describes accurately the simulation results, indicating negligible effective interactions. Analytical predictions for chemically identical blends or concentrated solution under bad solvent conditions do not exist in the literature.

### Micelle Size and Shape

Useful quantities to characterize the mixed micelles, formed by the aforementioned binary mixtures, are: the aggregation number  $N$ , the percentage content of constituent copolymers, the radii of gyration of the core  $\langle Rg^2 \rangle_{\text{core}}$  and of the whole aggregate  $\langle Rg^2 \rangle_{\text{micelle}}$  as well as the resulting thickness  $H$  and the shape anisotropies  $\kappa_{\text{micelle}}^2$ ,  $\kappa_{\text{core}}^2$ .

Shape anisotropy is defined as<sup>25,26</sup>

$$\kappa^2 = 1 - 3 \frac{I_2}{I_1^2} \quad (10)$$

where  $I_1$  and  $I_2$  are the first and the second invariants of the radius of gyration tensor.  $\kappa^2$  can take values ranging from 0 (sphere) to 1 (rod). The radius of the micelle core  $R_{\text{core}}$  can be calculated from its mean square radius of gyration by the relation  $R_{\text{gcore}}^2 = (3/5)R_{\text{core}}^2$ . The thickness of the mixed corona  $H$  can be obtained as the difference of the radii of the whole micelle and the core. All these properties were calculated on the most concentrated solutions with  $[X] = 0.12$ , where most aggregates are formed. Our results on the mass distributions of micelles, for different molar fractions of constituent copolymers in the mixtures, are illustrated in Figure 6, while the shape characteristics of the most probable micelles are summarized in Table 2. In the case of linear  $A_{63}B_{30}$ /star  $(A_{21})_3B_{30}$  mixtures the mass distribution depends on the molar fraction. Earlier, we found that the pure amphiphilics with miktoarm star architecture have sharper distribution peaked at a smaller value of preferential aggregation number  $N_p$  than the linear diblock counterparts.<sup>16</sup> By mixing the two copolymers we

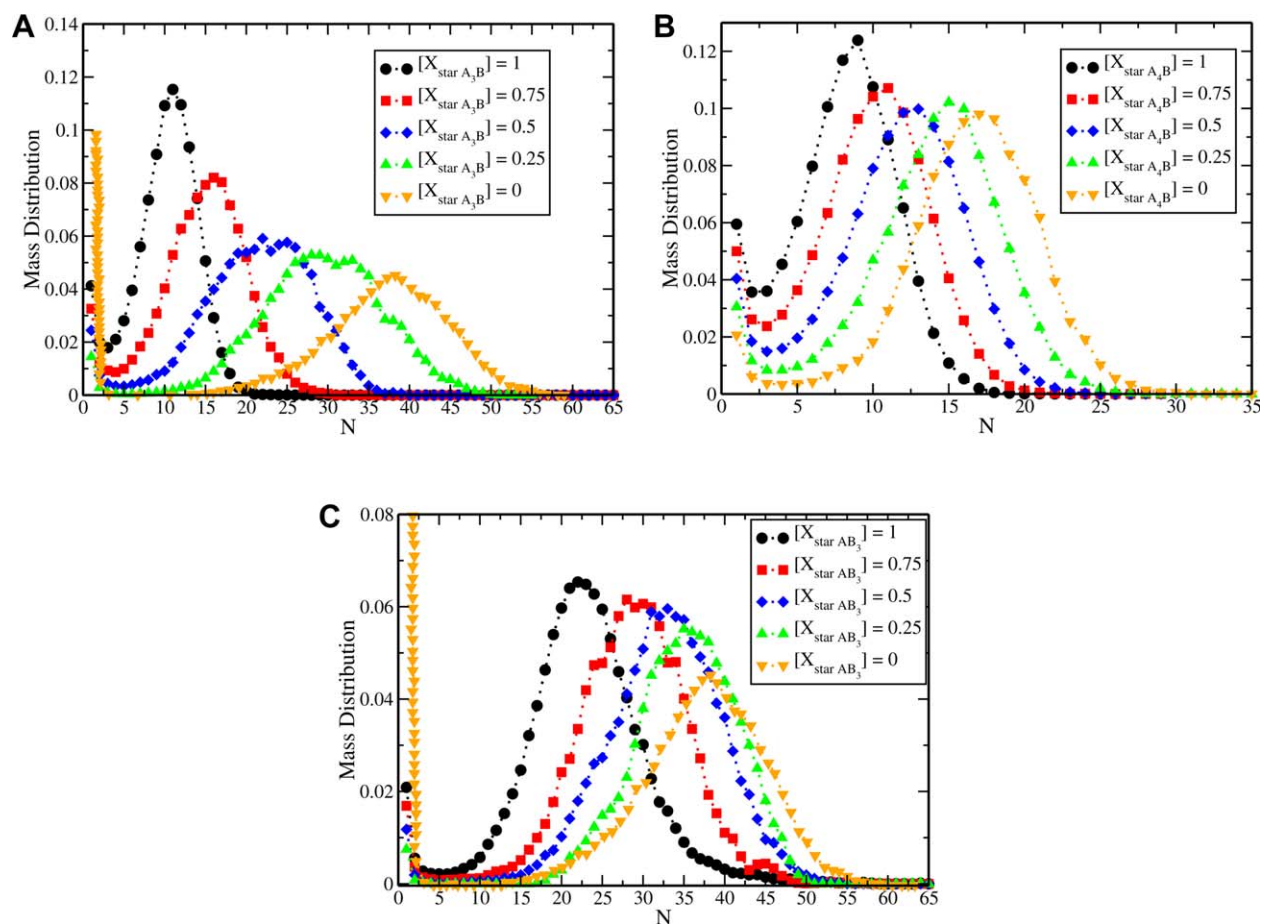


**FIGURE 6** Mass distributions of micelles in the mixtures: (a) linear  $A_{63}B_{30}$ /star  $(A_{21})_3B_{30}$ , (b) star  $(A_{32})_2B_{30}$ /star  $(A_{16})_4B_{30}$ , and (c) linear  $A_{63}B_{30}$ /star  $A_{63}(B_{10})_3$ , as a function of the aggregation number  $N_p$ . [Color figure can be viewed in the online issue, which is available at [wileyonlinelibrary.com](http://wileyonlinelibrary.com).]

noticed that one can interpolate between the two  $N_p$  limits. In Figure 7, the most probable aggregation numbers of micelles are plotted for mixtures with linear copolymer molar fraction  $[X_{\text{linear}}] = 0, 0.25, 0.5, 0.75, 1$ . The linear interpolation, mixing rule, describing the ideal mixtures is also presented. It can be observed that the most probable mixed micelle's aggregation number  $N_p$  within the standard deviation is marginally smaller than the respective value of the ideal mixture. For  $[X_{\text{linear}}] = 0.5$  mixture the most probable aggregation number is  $N_p = 22$ . Our simulation results have shown that these micelles contain 53% of star copolymer chains. The percentage content of the two copolymers in the mixed micelles with smaller or higher aggregation number than the preferential are also of some interest. The calculations indicate that 90% of the free chains are miktoarm star copolymers. For aggregates with  $N = 5, 10, 15, 20, 22, 26, 29$  this percentage becomes 21, 32, 43, 50, 53, 57, and 60%, respectively, indicating that micelles with  $N$  smaller than the preferential are enriched by the constituent copolymer having the higher cmc, while the larger micelles contains the constituent copolymer with the smaller cmc. The effective interactions reflect in a very small decrease in the aggregation number of preferential

micelles and should result in the nonrandom mixing between the linear and star solvophilic parts in the corona. To quantitatively describe, the mixing of linear and star solvophilic moieties in the corona we have calculated the radial distribution functions  $g(r)$  between the junction units of different linear-linear, star-star, and linear-star chains. The junction unit (Fig. 1) is the point where the solvophilic and solvophobic blocks of the copolymer connect. After the formation of the micelle, the junction points are located in the periphery of the core from where the solvophilic moieties consisting the corona originate. As can be observed from Figure 8(a) the peaks of the three different  $g(r)$  functions for the most probable micelle with  $N_p = 16$  and 22 for mixtures with  $[X_{\text{linear}}] = 0.25$  and 0.5, respectively, lie in different positions. Moreover, the peak of linear-linear  $g(r)$  is higher than the respective of linear-star  $g(r)$ , indicating larger population of linear chains as first neighbors. Thus, a nonrandom mixing of the copolymer chains in the corona is obtained. Additionally, snapshot analysis of the preferential micelles with  $N_p = 22$  for  $[X_{\text{linear}}] = 0.5$  have confirmed that the linear and the star chains are not randomly mixed and some domains, containing only one type of copolymers, are formed [Fig. 9(a)]. More or less, the content percentage of

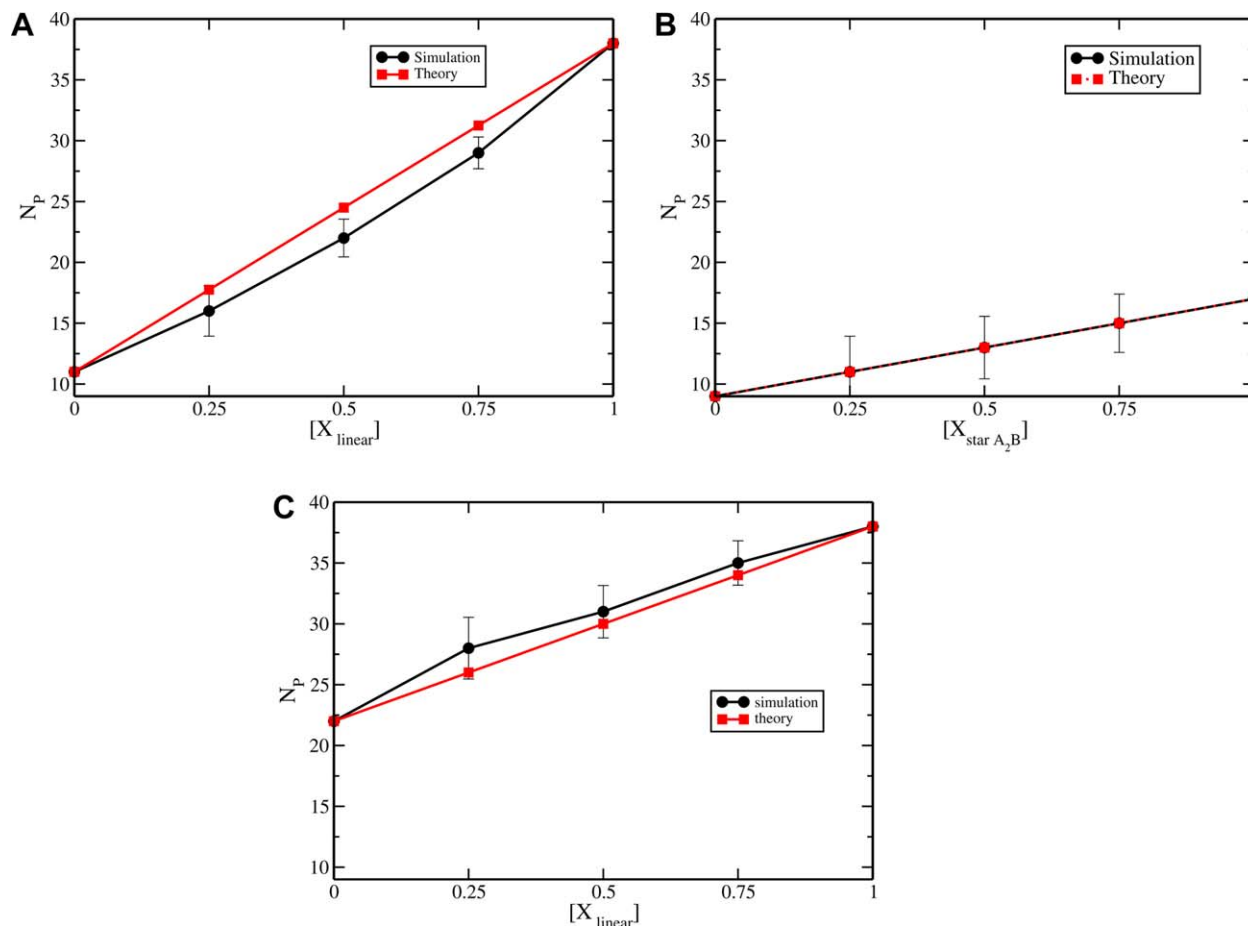


**FIGURE 7** The most probable aggregation numbers of micelles  $N_p$  for different mixtures: (a) linear  $A_{63}B_{30}$ /star  $(A_{21})_3B_{30}$ , (b) star  $(A_{32})_2B_{30}$ /star  $(A_{16})_4B_{30}$ , and (c) linear  $A_{63}B_{30}$ /star  $A_{63}(B_{10})_3$ . [Color figure can be viewed in the online issue, which is available at [wileyonlinelibrary.com](http://wileyonlinelibrary.com).]

one type of copolymer in the mixed micelle equals with the molar fraction of this constituent species in the solution. Snapshot analysis of the preferential mixed micelles with  $N_p = 16$ , at the molar fraction  $[X_{\text{linear}}] = 0.25$ , reveals that at

least two out of the four linear copolymer chains contained, are placed together in the corona. Similarly, from micelles with aggregation number 28, having seven star copolymer chains at  $[X_{\text{linear}}] = 0.75$  we found that some miktoarm star

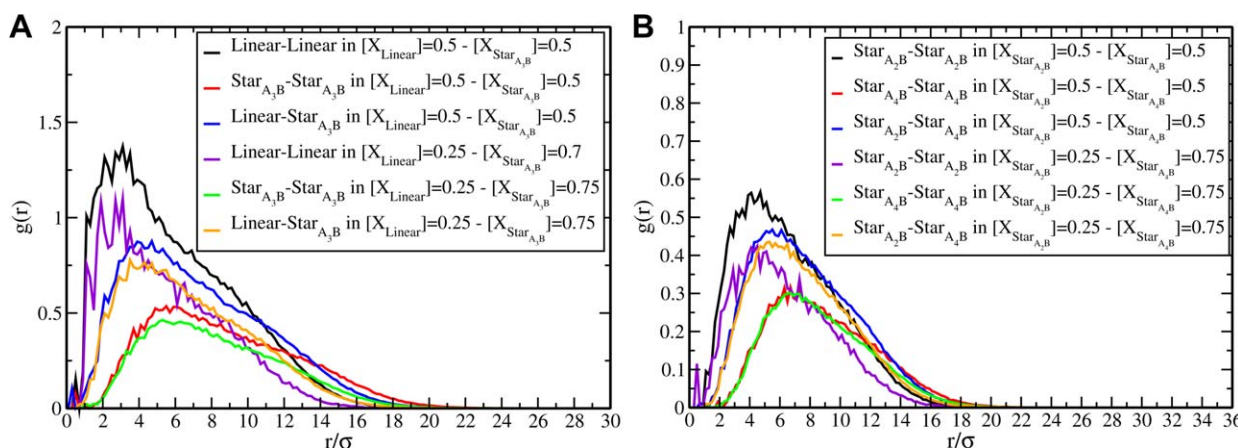


**FIGURE 8** Radial distribution functions of micelles with the most probable aggregation number for different copolymer mixtures: (a) linear  $A_{63}B_{30}$ /star  $(A_{21})_3B_{30}$  and (b) star  $(A_{32})_2B_{30}$ / star  $(A_{16})_4B_{30}$ . [Color figure can be viewed in the online issue, which is available at [wileyonlinelibrary.com](http://wileyonlinelibrary.com).]

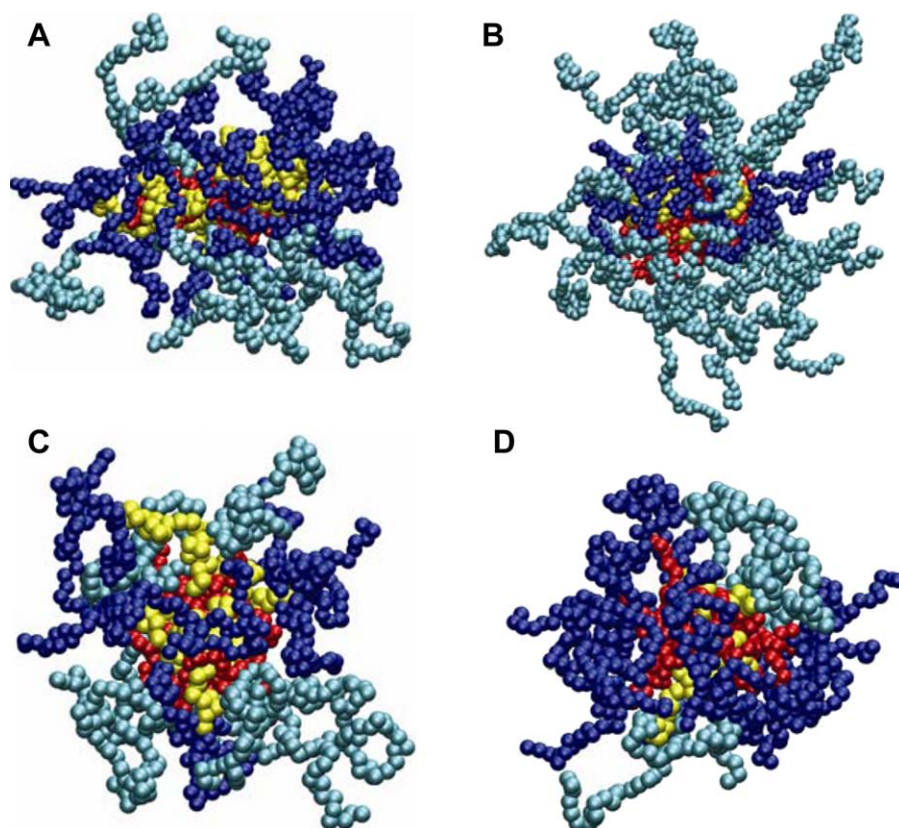


**FIGURE 9** Snapshots of micelles: (a)  $[X_{i,linear}] = 0.5$  with  $N_p = 22$ , (b)  $[X_{Star_{A_2B}}] = 0.25$  with  $N_p = 28$ , (c)  $[X_{Star_{A_2B}}] = 0.5$  with  $N_p = 13$ , (d)  $[X_{Star_{A_2B}}] = 0.25$  with  $N_p = 11$ . [Color figure can be viewed in the online issue, which is available at [wileyonlinelibrary.com](http://wileyonlinelibrary.com).]

copolymer chains contained, are placed together in the corona [Fig. 9(b)].

The shape of the pure linear micelles is more spherical than the pure miktoarm micelles, while the shape anisotropy parameter  $\kappa^2$  of preferential micelles increases progressively as the molar fraction  $[X_{star}]$  increases (Table 2), following more or less the mixing rule.

In star  $(A_{32})_2B_{30}$ /star  $(A_{16})_4B_{30}$  mixtures [Figs. 6(b) and 7(b)], having small difference in the number of star arms, the effective interactions are very small compared with the respective of linear/star mixtures according to analytical results of Vlahos and Kosmas.<sup>7–9</sup> Indeed the most probable aggregation number of mixed micelles  $N_p$  coincides with the predicted values of mixing rule as the molar fraction of star  $(A_{32})_2B_{30}$  increases. Similarly, the radial distribution functions  $g(r)$  between the junction units of star  $(A_{32})_2B_{30}$ -star  $(A_{32})_2B_{30}$ , star  $(A_{16})_4B_{30}$ -star  $(A_{16})_4B_{30}$ , and star  $(A_{32})_2B_{30}$ -star  $(A_{16})_4B_{30}$ , for the most probable micelle with  $N_p = 11$  and 13 for mixtures with  $[X_{(A_{16})_4B_{30}}] = 0.75$  and 0.5, respectively, are illustrated in Figure 8(b). The different peak positions and the higher peak of linear-linear  $g(r)$  distributions indicate nonrandom mixing of the copolymer chains in the corona. Snapshots have also shown a nonrandom mixing of both copolymers, in a variety of molar fractions [Figure 9(c,d)]. As expected, the mixed micelles are less spherical

than the respective, formed by the pure linear copolymers, and  $\kappa^2$  follows within the deviation the mixing rule (Table 2). Next, we study linear  $A_{63}B_{30}$ /star  $A_{63}(B_{10})_3$  mixtures where the constituent copolymers differ in the architecture of solvophobic part. As can be seen from Figures 6(c) and 7(c) the ideal model of eq 9 describes well the simulation results.

## CONCLUSIONS

The entropic effects in comicellization behavior of amphiphilic AB copolymers differing in chain architecture of solvophilic A or solvophobic B parts are studied by means of molecular dynamics simulations with Langevin thermostat. In particular, we studied linear/star, and star/star mixtures. The properties of interest are the critical micelle concentration, the mean aggregation number, the shape of the micelle, which is expressed by the shape anisotropy, the thickness of the corona, and the solvophobic core radius. The simulation results revealed that the cmc for linear/star mixtures shows a positive deviation from the ideal behavior, while in star/star and linear  $A_{63}B_{30}$ /star  $A_{63}(B_{10})_3$  mixtures where the constituent copolymers differ in the architecture of solvophobic part, the deviation is within the simulation uncertainty. The interaction parameters obtained from the activity coefficients could be attributed to the effective interactions between copolymers originated from the architectural asymmetry. These interactions are higher in the case of linear/star mixtures ( $u = 0.6$ )

and lower in star/star mixtures ( $u = 0.1$ ). These values are in qualitative agreement with Vlahos and Kosmas<sup>7–9</sup> analytical results for chemically identical blends. The effective interactions decrease slightly the micelles preferential aggregation number in linear/star mixtures while for the other mixtures the micelles preferential aggregation number can be satisfactorily predicted by the mixing rule. The calculation of radial distribution functions and the snapshot analysis reveals that the solvophilic parts of the copolymer chains are non-randomly mixed in the corona in all mixtures. Further theoretical and experimental studies are needed to clarify the issue of effective interactions, arising from the size and architectural asymmetry, on the micelle formation.

#### REFERENCES AND NOTES

- 1 M. Mackay, A. Tuteja, P. Duxbury, C. Hawker, B. Van Horn, Z. Guan, G. Chen, R. Krishan, *Science* **2006**, *311*, 1740–1743.
- 2 C. Greenberg, M. Foster, C. Turner, S. Corona-Galvan, E. Cloutet, R. Quirk, P. Butler, C. Hawker, *Polymer* **1999**, *40*, 4713–4716.
- 3 C. Greenberg, M. Foster, C. Turner, S. Corona-Galvan, E. Cloutet, R. Quirk, P. Butler, B. Hammouda, R. Quirk *J. Polym. Sci. Part B: Polym. Phys.* **2001**, *39*, 2549–2561.
- 4 T. Martter, M. Foster, T. Yoo, S. Xu, G. Lizzaraga, R. Quirk, P. Butler, *Macromolecules* **2002**, *35*, 9763–9772.
- 5 T. Martter, M. Foster, K. Ohno, D. Haddleton, *J. Polym. Sci., Part B: Polym. Phys.* **2002**, *40*, 1704–1708.
- 6 T. Martter, M. Foster, T. Yoo, S. Xu, G. Lizzaraga, R. Quirk, *J. Polym. Sci. Part B: Polym. Phys.* **2002**, *41*, 247–257.
- 7 C. Vlahos, M. Kosmas, *Polymer* **2003**, *44*, 503–507.
- 8 M. Kosmas, C. Vlahos, *J. Chem. Phys.* **2003**, *119*, 4043–4051.
- 9 C. Vlahos, M. Kosmas, *Macromolecules* **2004**, *37*, 9184–9190.
- 10 P. Theodorakis, A. Avgeropoulos, J. Freire, M. Kosmas, C. Vlahos, *Macromolecules* **2006**, *39*, 4235–4239.
- 11 P. Polanowski, J. K. Jeszka, *Langmuir* **2007**, *23*, 8678–8680.
- 12 B. Dong, R. Guo, L. T. Yan, *Macromolecules* **2014**, *47*, 4369–4379.
- 13 M. Murat, G. Grest, *Macromolecules* **1996**, *29*, 1278–1285.
- 14 S. Plimpton, *J. Comput. Phys.* **1995**, *117*, 1–19.
- 15 N. Suek, M. Lamm, *Langmuir* **2008**, *24*, 3030–3036.
- 16 C. Georgiadis, O. Moulto, L. N. Gergidis, C. Vlahos, *Langmuir* **2011**, *27*, 835–842.
- 17 O. Moulto, L. N. Gergidis, C. Vlahos, *Macromolecules* **2010**, *43*, 6903–6911.
- 18 A. Kalogirou, O. Moulto, L. N. Gergidis, C. Vlahos, *Macromolecules* **2014**, *47*, 5851–5859.
- 19 D. Levine, D. LeBard, R. DeVane, W. Shinoda, A. Kohlmeyer, M. Klein, *J. Chem. Theory Comput.* **2011**, *7*, 4135–4145.
- 20 L. Cheng, D. Cao, *Langmuir* **2009**, *25*, 2749–2756.
- 21 R. Nagarajan, *Langmuir* **1985**, *1*, 331–341.
- 22 S. Puvvada, D. Blankschtein, *J. Phys. Chem.* **1992**, *96*, 5579–5592.
- 23 G. K. Bourov, A. Bhattacharya, *J. Chem. Phys.* **2005**, *123*, 204712.
- 24 M. Zaldivar, R. G. Larson, *Langmuir* **2003**, *19*, 10434–10442.
- 25 D. N. Theodorou, U. W. Suter, *Macromolecules* **1985**, *18*, 1206–1214.
- 26 L. N. Gergidis, O. Moulto, C. Georgiadis, M. Kosmas, C. Vlahos, *Polymer* **2009**, *50*, 328–335.